

Electrical probing of cortical excitability in patients with epilepsy



Dean R. Freestone ^{a,b,*}, Levin Kuhlmann ^a, David B. Grayden ^a, Anthony N. Burkitt ^a, Alan Lai ^b, Timothy S. Nelson ^b, Simon Vogrin ^c, Michael Murphy ^c, Wendyl D'Souza ^c, Radwa Badawy ^a, Dragan Nesic ^a, Mark J. Cook ^c

^a Department of Electrical and Electronic Engineering, University of Melbourne, Parkville, VIC, 3010, Australia

^b Bionics Institute, East Melbourne, VIC, 3002, Australia

^c St. Vincent's Hospital Melbourne, Fitzroy, VIC, 3065, Australia

ARTICLE INFO

Article history:

Received 5 July 2011

Revised 4 September 2011

Accepted 5 September 2011

Keywords:

Cortical excitability

Electrical probing

Intracranial

Electroencephalography

Seizure prediction

ABSTRACT

Standard methods for seizure prediction involve passive monitoring of intracranial electroencephalography (iEEG) in order to track the 'state' of the brain. This paper introduces a new method for measuring cortical excitability using an electrical probing stimulus. Electrical probing enables feature extraction in a more robust and controlled manner compared to passively tracking features of iEEG signals. The probing stimuli consist of 100 bi-phasic pulses, delivered every 10 min. Features representing neural excitability are estimated from the iEEG responses to the stimuli. These features include the amplitude of the electrically evoked potential, the mean phase variance (univariate), and the phase-locking value (bivariate). In one patient, it is shown how the features vary over time in relation to the sleep–wake cycle and an epileptic seizure. For a second patient, it is demonstrated how the features vary with the rate of interictal discharges. In addition, the spatial pattern of increases and decreases in phase synchrony is explored when comparing periods of low and high interictal discharge rates, or sleep and awake states. The results demonstrate a proof-of-principle for the method to be applied in a seizure anticipation framework.

This article is part of a Supplemental Special Issue entitled The Future of Automated Seizure Detection and Prediction.

© 2011 Elsevier Inc. All rights reserved.

1. Introduction

The ability to predict or anticipate epileptic seizures has the potential to revolutionize the treatment of epilepsy by enabling the application of preventative therapy. Furthermore, successful anticipation¹ of seizures will provide dramatic increases in the quality of life by potentially providing a warning system for the millions of people worldwide with uncontrolled seizures.

Over recent decades, the majority of seizure prediction algorithms that have been proposed in the literature have been developed using passively recorded intracranial electroencephalography (iEEG). Although most methods are mathematically quite varied, the majority are conceptually similar and focus on measuring the degree of order or complexity observed in the electrical fields of the brain. A

decrease in complexity or disorder is thought to be indicative of abnormal hyper-synchronous dynamics associated with a pre-seizure time period. Earlier algorithms involved estimating entropy, correlation dimension, and short-term Lyapunov exponents [1–5].

The research focus has shifted to include synchronization analysis after the aforementioned methods failed to deliver repeatable results among different groups [6–9]. These synchrony-based algorithms have shown promise in certain patient groups, but they have not delivered sufficiently reproducible outcomes and, therefore, have not provided satisfactory clinical performance [10,11].

A major limiting factor in the development and validation of seizure prediction algorithms has been the lack of long-term iEEG data. Typically, iEEG data is captured from epilepsy patients undergoing planning for resective surgery. The monitoring period is normally limited to 1–2 weeks due to risks of infection and other complications. Therefore, it is not uncommon for only a small number of seizures, which may be atypical due to drug withdrawal and surgical recovery, to be recorded. The small number of atypical seizures combined with the heterogeneity of epileptic pathologies makes seizure prediction algorithm development difficult.

Another difficulty faced by seizure prediction developers is the interpretation of the spontaneously recorded iEEG signal. Although

* Corresponding author at: Department of Electrical and Electronic Engineering, University of Melbourne, Parkville, VIC, 3010, Australia. Fax: +61 383447412.

E-mail address: deanrf@unimelb.edu.au (D.R. Freestone).

URL: <http://www.neuroeng.unimelb.edu.au> (D.R. Freestone).

¹ Seizure anticipation often refers to estimating the instantaneous likelihood of seizure occurrence where seizure prediction often refers to forecasting a seizure within a set time period. In this paper we use the terms interchangeably.

the iEEG is perhaps the best available clinical tool for recording the spatiotemporal dynamics of the human brain, the problem of uncovering the generators of the electrical fields is still considered ill-posed. For example, most experimental paradigms in cognitive neuroscience require averaging EEG responses to many (hundreds of) stimuli to reveal networks involved in specific brain function. This is because the subtle dynamics in the responses are hidden in background fluctuations of ongoing brain activity.

In this paper, a framework is presented for obtaining electrical-evoked potentials (EEPs) from the epileptic foci. The EEPs enable averaging out of the spontaneous fluctuations of ongoing brain processes. After averaging, the iEEG provides an indication of the brain's ability to respond to stimulation, which is a reflection of cortical excitability. By periodically tracking EEPs, we can monitor cortical excitability and potentially develop more robust seizure anticipation methods.

1.1. Probing for cortical excitability

1.1.1. Previous studies

Probing the brain refers to applying a stimulus to the brain to measure the transient or steady-state response in order to quantify excitability, where a large response indicates high excitability. In this paper, we use the term excitability in a non-specific manner, where, for example, high excitability may result from low levels of inhibition. It is hypothesized that changes in excitability are a necessary condition for epileptic seizures. Therefore, tracking excitability may lead to a clinically effective seizure prediction method. The notion of using a probing stimulus to detect critical changes in complex dynamical systems has been applied extensively to other systems [12], but represents a significant paradigm shift in the study of brain dynamics and the field of seizure prediction.

Since the pioneering work of Penfield [13], electrical stimulation of the brain is the gold standard for cortical mapping in surgical planning for epilepsy patients. The cortical mapping allows clinicians to map the spatial aspects of both functional and pathologic tissue by observing behavioral responses to stimuli. More recently, iEEG responses to single pulse electrical stimulation (SPES) have been used to better identify reverberant cortical circuits associated with epileptic pathologies [14–17]. The success in using an input stimulus in mapping the spatial aspects of the epileptic pathologies motivates using an input to map the temporal transitions from normal dynamics to seizures.

The first reports (to the authors' best knowledge) of probing the brain for epileptic seizure anticipation used magnetoencephalographic (MEG) responses to intermittent photonic stimulation to measure cortical excitability [18]. This methodology was specifically targeted to patients with photosensitive epilepsy. Using this approach, the authors developed a measure named the relative phase clustering index (rPCI) to quantify changes in excitability. With this measure, they showed that phase clustering in a harmonic of the stimulus frequency (gamma band) increased as a function of the time to next seizure.

The rPCI measures the phase dispersion in the iEEG response to electrical stimulation, assuming a stationary sinusoidal steady-state response. The rPCI gives a measure of phase entrainment of the iEEG in the harmonics of the stimulation frequency, capturing nonlinear phenomena. This feature is only valid for steady-state responses with a stationary frequency, making application to single-pulse stimulation impractical.

The rPCI methodology was extended to a more general scenario using a sub-threshold electrical stimulus as a probe [19]. This study demonstrated that the time to the next seizure could be reliably predicted from the rPCI measure in a small group of MTLE patients. Furthermore, this study demonstrated how this measure could be used to localize epileptic networks. Due to the limited number of patients, Kalitzin et al. acknowledged that the results only provide a proof of principle for this approach and further validation of the approach is required.

Another study used iEEG responses to electrical stimulation to determine cortical excitability in order to monitor neural plasticity

associated with a seizure onset zone in epilepsy surgery patients [20]. Although this measure was not used to track temporal changes associated with transitions from normal to a pre-seizure state, the study further demonstrates the potential for using the brain's responses to electrical stimulation to monitor cortical excitability. Further to this, a recent review discussing the use of direct electrical stimulation of the brain as an under-utilized tool for epilepsy research noted the need for more clinical investigations into the use of electrical stimulation for seizure prediction [21].

1.1.2. Theoretical motivation

Recent theoretical evidence suggests an active approach is required for seizure anticipation [22]; it was shown that changes in excitability in a computational model of TLE could only be tracked when an active paradigm was employed. Further theoretical evidence of the requirement of an active approach for seizure prediction is provided by O'Sullivan-Greene et al. [23], who showed that the failure of EEG-based seizure prediction algorithms is not necessarily because the correct EEG feature has not been found to create the typical machine learning expert system, but rather that seizure precursors are not observable from the passively recorded EEG signal itself. That is, the passive EEG only allows the observation of a very small fraction of the underlying generators of brain activity. This indicates that seizure anticipation from passive EEG is unlikely to succeed. However, it was shown (through computer simulation) that the clever use of a probing stimulus can extract information from the EEG to facilitate seizure anticipation, even if the underlying neurodynamics cannot be observed in the passive EEG measurements [24]. Further theoretical justification for the use of probing stimulation was provided by Kalitzin et al. [25], who showed that a small perturbation of the cortical dynamics may enable the measurement of the likelihood of seizure occurrence.

1.1.3. Other measurement modalities

Electrical stimulation is not the only method suitable for probing the brain to track excitability. For example, it has been demonstrated that cortical excitability in patients with idiopathic generalized epilepsy or focal epilepsy (including TLE) can be measured by probing the brain using transcranial magnetic stimulation (TMS) [26]. Stimulations were delivered to the motor cortex and excitability was evaluated using electromyography (EMG). It was found that patients whose seizures were resistant to drug therapies had hyper-excitable networks. Furthermore, excitability was elevated in a pre-seizure period. In similar research, using an acoustic auditory stimulus, Lin et al. found significant changes in the timing of event-related synchrony around the time periods where seizures occurred [27]. It was found that epileptic tissue synchronized faster than that of normal tissue, implying pre-seizure hyper-excitable. Other modalities for tracking pre-seizure hyper-excitable include near infrared spectroscopy (NIRS) [28] and functional magnetic resonance imaging (fMRI) [29]. The major benefit in using electrical stimulation with iEEG over other modalities is the ability to incorporate the stimulation and measurement system into an implantable seizure advisory/control device. A benefit in using electrical stimulation over a sensory-evoked potential is the ability to excite tissue without generating a percept that may be poorly tolerated over long periods of time.

2. Method

2.1. Patients

The iEEG data used in this study were collected from two patients undergoing evaluation for the surgical resection of epileptic foci at St. Vincent's Hospital in Melbourne, Australia. Data were collected under ethics approval from St. Vincent's Human Research Ethics Committee (HREC-A 006/08). The standard clinical practice for epilepsy related surgery involves a diagnostic period of 1 week, where

iEEG electrodes are implanted subdurally, directly on the surface of the brain. Images of the location of the subdural grid electrodes for each of the patients are shown in Fig. 1. These electrodes are used to map pathological brain tissue by recording abnormal oscillations in the electrical fields of the brain. In addition, the electrodes facilitate spatial mapping of important functional brain tissue, such as speech and motor control, by applying electrical stimuli and observing the behavioral responses. All data were collected via intracranial grids with platinum disk electrodes (Ad-Tech Medical, Racine WI). The data from Patient 1 were acquired from an 8×4 array with regular spacing of 10 mm in both x - and y -directions. The data from Patient 2 were acquired from a 15×8 array of electrodes with regular spacing in the x -direction of 5 mm and 10 mm in the y -direction. All iEEG data were marked independently by an experienced neurophysiologist who was blinded to the signal analyses.

During the week-long monitoring period, both patients experienced multiple seizures. However, during the experimental period involving the probing, Patient 1 had one clinical seizure and Patient 2 had no clinical seizures. Although no clinical seizures occurred for Patient 2, there was a time period where many interictal epileptic discharges occurred. Therefore, we compared the number of discharges to the iEEG features in the probing analyses.

Figs. 2(a) and (b) show examples of iEEG seizure onsets from both Patients 1 and 2, respectively. As seen in the examples, both patients had focal seizure onsets.

2.2. Data acquisition and stimulation

In parallel to the standard clinical procedure, the electrical stimulation protocol was conducted. The electrical stimuli were delivered by a Grass S88x neurostimulator (Astro-Med, West Warwick, RI) and consisted of single bipolar, biphasic pulses delivered in groups of 100, with each pulse separated by 3.01 s. Therefore, each block of stimulations lasted for approximately 5 min. A rest period of 5 min was included between each stimulation group. This pattern of 5 minute 'on', 5 minute 'off' was continuously repeated over the course of approximately 23 and 13 h for Patients 1 and 2, respectively. The pulse width was 100 μ s with current intensity of 2 mA. This current intensity yielded measurable responses in the iEEG with no behavioral percept. The resulting response was a transient deflection in the iEEG signal as seen in Fig. 3. To be clear, the responses were not epileptic after-discharges. The current intensity yielded a charge/phase of 0.2 μ C/phase and a charge density of approximately 0.4 μ C/phase/ cm^2 (for an electrode diameter of 4 mm). This charge density is approximately 2 orders of magnitude below the well-documented safety limits of 30 μ C/phase/ cm^2 [30,31,32,33]. Stimuli were targeted to low-impedance electrodes that were not in direct

contact with the cerebral vasculature. An example of the EEP from Patient 1 is shown in Fig. 3. For Patient 1, stimuli were targeted to the suspected epileptic foci and surrounding tissue. For Patient 2, stimuli were directed to a more remote site. The locations of the epileptic foci and stimulation sites can be seen by the color coding of electrodes in Fig. 1.

The iEEG was sampled at a rate of 5 kHz and the EEG system (Synamps2 Compumedics, Abbotsford Vic.) allowed for recording from a DC level (24-bit resolution), meaning transient responses to stimuli could be observed.

2.3. Signal processing

When eliciting an observable response in the iEEG from a single pulse electrical stimulation, the recording resembles the early component of an evoked response from an auditory (click) or visual (flash) evoked experiment. Naturally occurring evoked responses are thought to be due to a phase resetting of the cortical oscillations [34]. Therefore, in addition to studying the amplitude of evoked potentials, phase-locking measures are a logical choice for quantifying the response that is induced when using electrical stimulation.

Three features are used in this paper to quantify the response to electrical stimulation. The first is the amplitude of the EEP; the second is a novel measure, the mean phase variance (MPV); and the third is the well known phase-locking value (PLV) or otherwise known as mean phase coherence. The MPV is a univariate measure of the inter-stimulus variation in the unwrapped instantaneous phase (IP). Essentially, the measure captures the variation in the instantaneous frequency of the responses. The motivation for using this measure is that we suspected that the MPV would increase as hyper-excitable pathological tissue begins to drive and exert control over the normal oscillatory activity of the cortex. The PLV is included because it is widely used in the seizure prediction literature.

2.3.1. Pre-processing

Pre-processing and signal conditioning are required to ensure that noise has a minimal effect on the analysis. The first pre-processing step was to identify and exclude channels that had poor signal quality via visual inspection. Next, all epochs were visually inspected for artifact. Corrupted epochs were excluded. This included epochs where epileptic spikes were present in the stimulus response period. Note, if spontaneous epileptic discharges were present in the stimulus response period, which is the time window of the feature extraction (5–100 ms post-stimulation) of a particular epoch, then it was excluded from the analyses.

Next, 10 samples centered around each stimulus were removed from the time series, and reintroduced using linear interpolation.

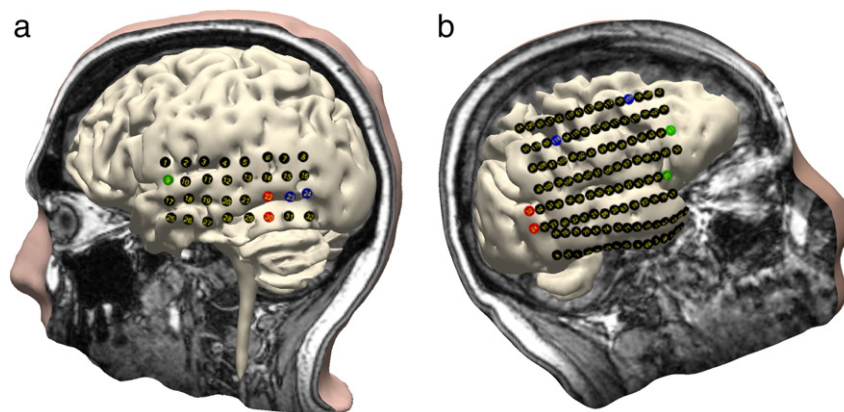


Fig. 1. Structural MRI co-registered with CT scan to show grid electrode implantation locations. For both patients the electrodes over the epileptic focus are plotted in red, the channels used for the probing stimulus are plotted in blue, and the channels used as a reference are plotted in green. (a) Patient 1 with a 32-channel grid electrode. (b) Patient 2 with a 120-channel grid electrode.

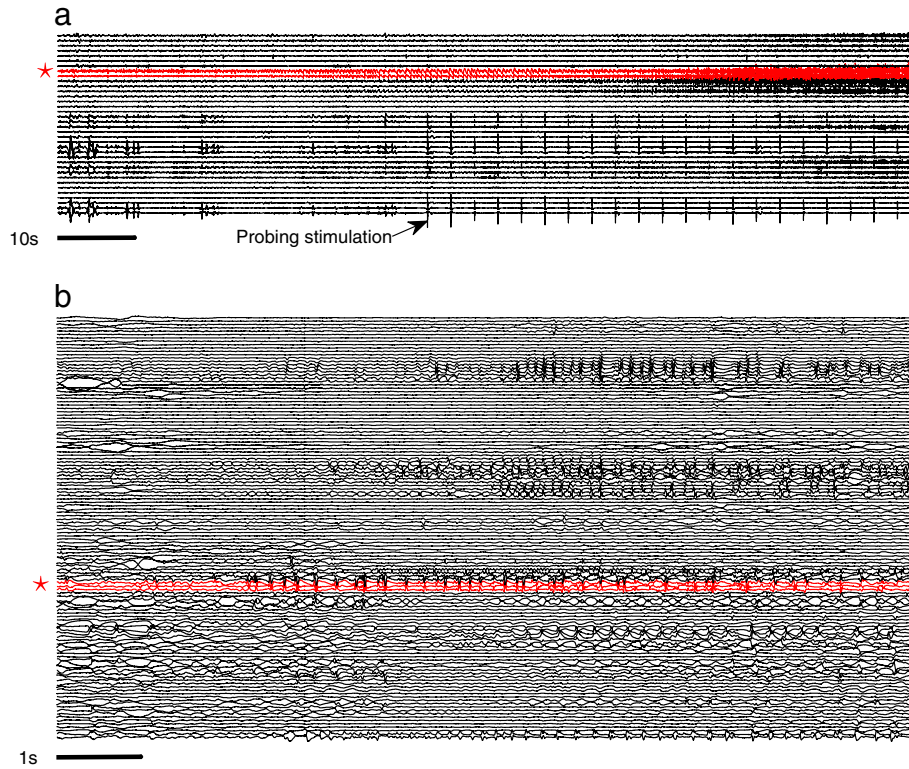


Fig. 2. Seizure onsets recorded with iEEG from two patients. The iEEG data have been re-referenced to a differential montage. The red stars to the left of the iEEG plots indicate the focal channels, which are also plotted in red. (a) Seizure onset from Patient 1. The plot shows 110 s of data demonstrating a gradual seizure onset. A block of probing stimulations coincidentally commenced after the seizure onset. (b) Seizure onset from Patient 2.

This removed the majority of the stimulation artifact [35]. Next, the data were smoothed using a 10th-order moving average filter. This step reduced sharp fluctuations and discontinuities (from residual stimulation artifact) in the signal that cause ringing when digital filtering is applied. The data were then 50-Hz notch filtered and low-pass filtered (cut-off $f_c = 95$ Hz) in the reverse time direction using a 2nd-order Butterworth filter. Filtering in the reverse time direction ensured that any ringing induced by residual discontinuities from the stimulation appeared in the pre-stimulus time period (see Fig. 3 for example). The data were then resampled from 5 kHz to 1 kHz and re-referenced to a differential montage, to remove common-mode interference and the effect of the reference electrode. Only unique combinations of neighboring pairs in the x and y directions (above, below, left, or right) of the electrodes, where both electrodes gave good signal quality, were used in the new montage.

Following the pre-processing and filtering steps, the data were epoched about the time of stimulations. Time intervals from 5 ms to 100 ms post-stimulation were used for analysis. Blocks of stimulation where greater than 50% of the epochs had obvious artifacts were

excluded in order to gain reliable statistics from the interaction measures. For each accepted block, this approach yielded at least 50 responses to stimulation to form the excitability measures.

2.3.2. Electrical-evoked potential (EEP) amplitude

The amplitude of the EEP was quantified as

$$\beta_\alpha = \max_n \frac{1}{\Gamma} \sum_\gamma y_{\alpha,\gamma}(n) - \min_n \frac{1}{\Gamma} \sum_\gamma y_{\alpha,\gamma}(n), \quad (1)$$

where $y(n)$ is the preprocessed iEEG, α indexes the channels (in the differential montage), γ indexes the Γ (non-corrupted) stimulations in each 10-minute period, and n indexes the temporal sampling in the stimulation response period.

2.3.3. Instantaneous phase (IP) estimation

Estimation of the IP is required to compute the MPV and PLV measures. To estimate the IP, data must be filtered into narrowband or semi-narrowband components [36]. Accordingly, semi-narrowband

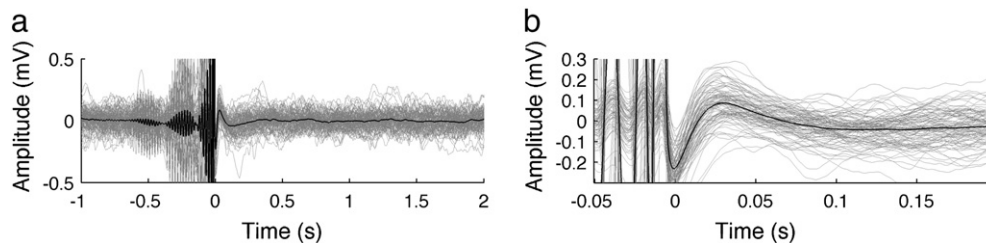


Fig. 3. Example of the electrical evoked potential from Patient 1. The thin gray lines show individual stimulation responses and the thick black line shows an average over the 100 stimuli in the stimulation block. Stimuli were delivered at $t = 0$. The ringing in the pre-stimulus period is an artifact from digital filtering in the reverse time direction resulting from small discontinuities induced by stimulation. (a) Three seconds of data around the stimuli. (b) A zoomed view of the electrical evoked potential.

components of the iEEG were extracted via bandpass filtering. The center frequencies for the results presented in this paper were 15 and 25 Hz for Patients 1 and 2, respectively, with a bandwidth of 10 Hz. Analysis with other frequency ranges was conducted in preliminary analyses. The frequency ranges presented in this paper were chosen because they provided a good contrast in the extracted features between epileptic and non-epileptic excitability estimates. The instantaneous phase, $\phi(n)$, can be estimated by

$$\phi_{\alpha,\gamma}(n) = \arctan\left(\frac{\mathcal{H}\tilde{y}_{\alpha,\gamma}(n)}{\tilde{y}_{\alpha,\gamma}(n)}\right), \quad (2)$$

where $\tilde{y}_{\alpha,\gamma}(n)$ is the pre-processed and bandpass filtered iEEG and the operator \mathcal{H} denotes the Hilbert transform. Prior to computing the phase variance, the phase was shifted such that $\phi_{\alpha,\gamma}(0)=0$ and the phase was unwrapped.

2.3.4. Mean phase variance (MPV)

Given the phase estimate, $\phi(n)$, the phase variance, $\sigma^2(n)$, for a given iEEG channel is

$$\sigma_{\alpha}^2(n) = \frac{1}{\Gamma} \sum_{\gamma=1}^{\Gamma} \left(\phi_{\alpha,\gamma}(n) - \bar{\phi}_{\alpha}(n) \right)^2, \quad (3)$$

where $\bar{\phi}_{\alpha}(n)$ is the mean of $\phi_{\alpha,\gamma}(n)$ over the Γ stimulations within the stimulation group. To reduce phase variance to a scalar quantity,

the mean over the stimulus response period is taken. This gives the MPV:

$$\chi_{\alpha} = \frac{1}{N} \sum_{n=1}^N \sigma_{\alpha}^2(n), \quad (4)$$

where N is the number of samples in the response period.

2.3.5. Phase-locking value (PLV)

Given an estimate of the instantaneous phase of the iEEG, $\phi_{\alpha,\gamma}(n)$, phase-locking between two signals, a and b , is defined as

$$\phi_{a,\gamma}(n) - \phi_{b,\gamma}(n) = \text{constant}, \quad (5)$$

and phase entrainment is defined as

$$\phi_{a,\gamma}(n) - \phi_{b,\gamma}(n) < \text{constant}. \quad (6)$$

The phase synchrony measures are evaluated using circular statistics. The PLV for a single trial is defined as

$$PLV_{a,b,\gamma} = \frac{1}{N} \left| \sum_n \exp(i(\phi_{a,\gamma}(n) - \phi_{b,\gamma}(n))) \right| \quad (7)$$

$$= 1 - CV, \quad (8)$$

where $i = \sqrt{-1}$ and CV denotes circular variance [37]. Eq. (7) is the standard form used in many seizure prediction algorithms (see [10])

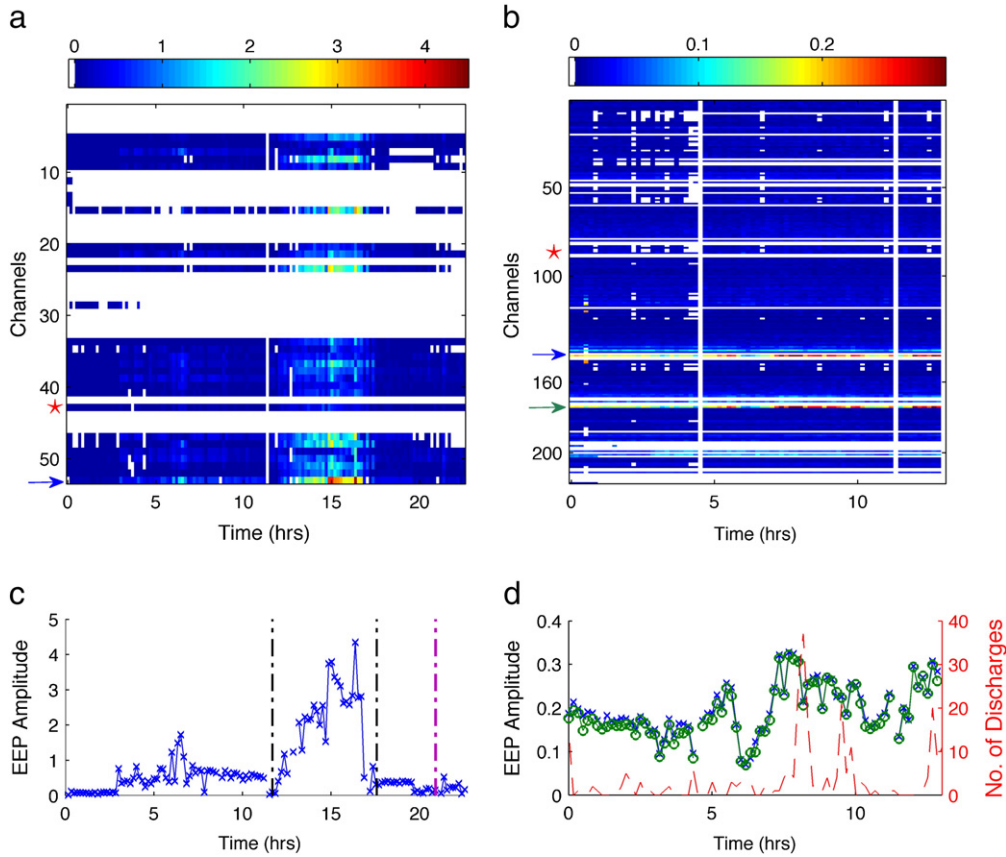


Fig. 4. Results from the EEP amplitude analysis. (a) and (b) The EEP amplitude time series for all available channel combinations in the differential montage for Patients 1 and 2, respectively. The colorbar indicates magnitude of the EEP amplitudes (white indicates rejected stimulation blocks), the vertical dimension indexes channels in the differential montage and the horizontal dimension represents time (hours). (c) EEP amplitude time series for a selected channel from Patient 1 plotted with markers of the sleep–wake period (between vertical black dash–dot lines) and seizure onset (vertical purple dash–dot lines). (d) EEP amplitude time series for 2 channels from Patient 2 plotted with the interictal discharge rate (red dashed line). The colored arrows alongside the images in (a) and (b) are color-matched to the EEP amplitude time series shown in (c) and (d), respectively.

for a review). A more robust form of the PLV that is used in this paper, defines phase synchrony between the averaged EEPs from two paired channels:

$$PLV_{a,b} = \frac{1}{\Gamma N} \sum_n \left| \sum_{\gamma} \exp(i(\phi_{a,\gamma}(n) - \phi_{b,\gamma}(n))) \right|. \quad (9)$$

3. Results

3.1. Results from EEP amplitude analyses

The temporal evolution of the EEP amplitudes is shown in Fig. 4 for both patients. Parts (a) and (b) of the figure show the EEP amplitudes for all available channels in the differential montage for Patients 1 and 2, respectively. The red stars to the left of the figures indicate the position of the focal channels in the montage (as shown in Fig. 2). Parts (c) and (d) show a selection of channels, comparing the extracted features to epileptic events and a sleep–wake period for Patient 1.

Figs. 4(a) and (c) (Patient 1) show that the EEP amplitude increases during the sleep period, but does not appear to change significantly at, or in the lead up to, the seizure. The change in the EEP amplitude is widespread across the majority of iEEG recording sites. The largest change in the EEP amplitude, shown by the time series in Fig. 4(c), occurred at an electrode location adjacent to the stimulation site away from the epileptic focus. This indicates that the pathol-

ogy was not the determining factor in the temporal changes observed during the sleep–wake cycle.

For Patient 2, localized changes in the EEP amplitude coincided with the high interictal spike rate. These changes remained very localized to the probing stimulation site, which was remote to the site of seizure onset. The majority of cortical regions appear to give a relatively constant response.

3.2. Results from MPV analyses

Fig. 5 provides the results from the MPC analyses. The arrangement of the plots follows the same format as the EEP amplitude analyses in Fig. 4. In contrast to EEP amplitude analysis, the figure demonstrates a distinct relationship between the MPV and the epileptiform activity. Figs. 5(a) and (c) illustrate that for Patient 1, the average (across channels) MPV decreases in the lead up to the seizure. The average MPV is also higher during the sleep period and the post-ictal period, demonstrating the potential for the MPV feature to measure excitability and anticipate seizures.

Fig. 5(b) indicates that the MPV varies in a much more widely distributed manner compared to the EEP amplitude for Patient 2. Fig. 5(d) demonstrates that the selected channels show a strikingly similar profile to the discharge rate. Note, if epileptic discharges were present in the stimulus response period (5–100 ms post-stimulation) of a particular epoch, then it was excluded from the analyses. Therefore, the result indicates that in this case the probing framework is predictive of epileptic behavior.

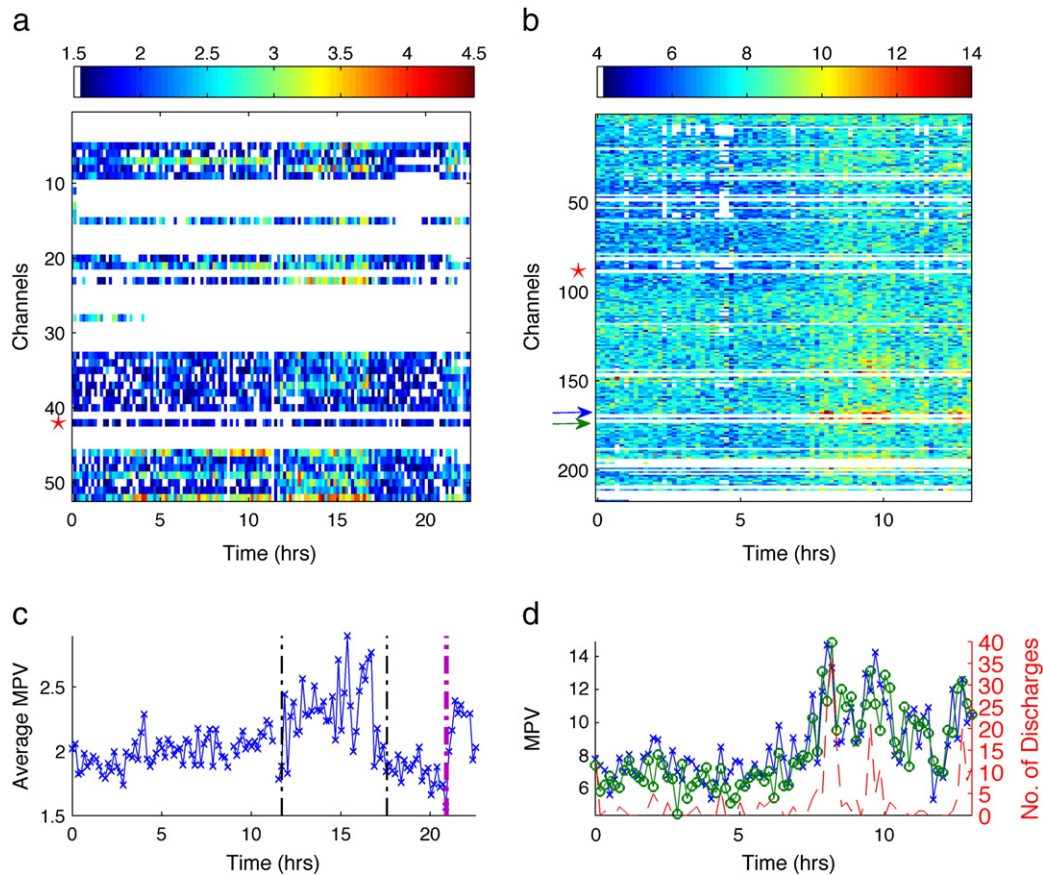


Fig. 5. Results from the MPV analyses. Univariate MPV time series for both patients for all channels. (a) and (b) The MPV time series for Patients 1 and 2, respectively. In (a) and (b) the colorbar indicates MPV magnitude (white indicates rejected stimulation blocks), the vertical dimension indexes channels in the differential montage and the horizontal dimension represents time (hours). (c) MPV time series averaged across all channels for Patient 1 plotted with markers of sleep onset and offset (between vertical black dash-dot lines) and the onset of a seizure (vertical purple dash-dot line). (d) The MPV time series for 2 channels from Patient 2 plotted against the interictal discharge rate (red dashed line). The blue and green arrows alongside the image in (b) indicate the channels that correspond to the blue and green MPV time series in (d), respectively.

In a similar manner to the EEP amplitude analysis, the largest changes in the MPV relative to the epileptic events occurred more focally to the stimulation site than the site of seizure onset in both patients.

3.3. Results from PLV analyses

The PLV was calculated for all unique channel combinations of the differential montage (excluding self relationships). This yielded 2704 and 47,089 time series for Patients 1 and 2, respectively. The high dimensionality of the data prohibits display in a sensible manner given the space limitations. Therefore, the dimensionality was reduced by selecting the PLVs that had the largest change between time periods of interest. For Patient 1 the time periods were from 0 to 10 h and 12 to 17 h, and for Patient 2 from 0 to 7 h and 7 to 13 h. The PLVs for each channel were averaged over these time periods and difference was taken. A threshold was set at 0.22, and the channels that had an absolute difference greater than the threshold were kept for display. This allowed for both increases and decreases. The threshold value resulted from a trade-off between providing clarity and detail in the figures.

Fig. 6 provides the results from the PLV analysis. For both patients, there were widespread changes in the PLV over time relative to the epileptic events and sleep–wake cycle.

The analyses demonstrate that the PLV feature captures changes in sleep–wake cycle, epileptic discharge rate, and the seizure. For Patient 1, Figs. 6(a) and (c) strikingly illustrate that there are both dramatic decreases and increases in the PLV value when

transitioning between sleep and wake periods. There are also large changes in PLV when transitioning between the pre-ictal and post-ictal periods.

Figs. 6(b) and (d) demonstrate for Patient 2 that there are increases or decreases in the PLV value when comparing periods with low versus high interictal discharge rates.

The spatial pattern of these PLV changes is captured for both patients in Fig. 7. Fig. 7(a) shows the magnitude of increases and decreases in PLV between channel pairs for Patient 1 for the transition from the wake to the sleep state. Fig. 7(b) shows the magnitude of increases and decreases in PLV between channel pairs for Patient 2 for the transition from periods of low to high interictal discharge rates. In both Figs. 7(a) and (b) it is apparent that the greatest changes in PLV occurred away from the focal channels. Note, the network map for Patient 1 should be interpreted with care due to the number of channels that were rejected from the analysis. For Patient 2, the greatest changes in synchrony levels were between the stimulation electrodes, away from the site of seizure onset. Nevertheless, the PLV showed changes coinciding with interictal discharges, demonstrating the utility of using the EEP-based PLV feature to distinguish sleep/wake and discharge states.

4. Discussion

This paper introduces a new method for tracking cortical excitability by using an electrical probing stimulus. This work builds on other studies that use an active approach for measuring excitability,

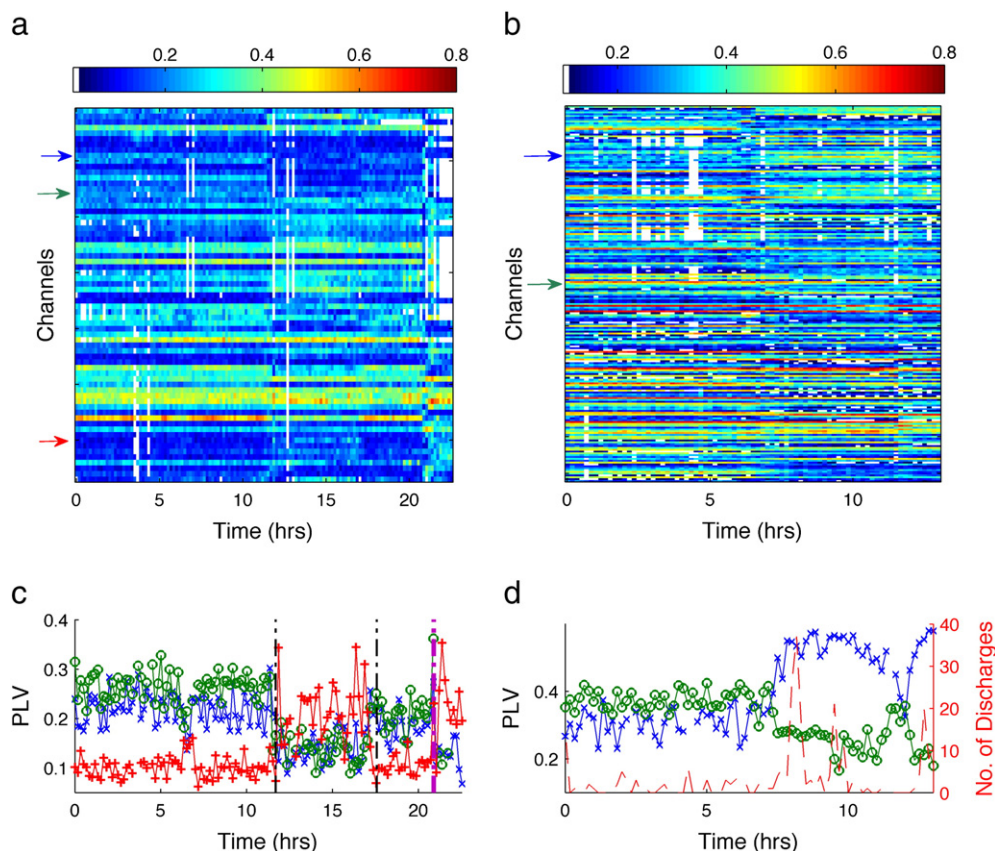


Fig. 6. Bivariate PLV time series for both patients for select channels. (a) and (b) The PLV time series for Patients 1 and 2, respectively. In (a) and (b) the colorbar indicates PLV magnitude (white indicates rejected stimulation blocks), the vertical dimension indexes selected channel pairs and the horizontal dimension represents time (hours). (c) PLV time series for select channel pairs for Patient 1 plotted with the times of sleep onset and offset (between vertical black dash-dot lines) and the onset of a seizure (vertical purple dash-dot line). (d) PLV time series for select channel pairs from Patient 2 plotted against the interictal discharge rate (red dashed line). The colored arrows alongside the images in (a) and (b) are color matched to the PLV time series shown in (c) and (d), respectively. The channel pairs were chosen that show the largest change in PLV between wake (0–10 h) and sleep states (12–17 h).

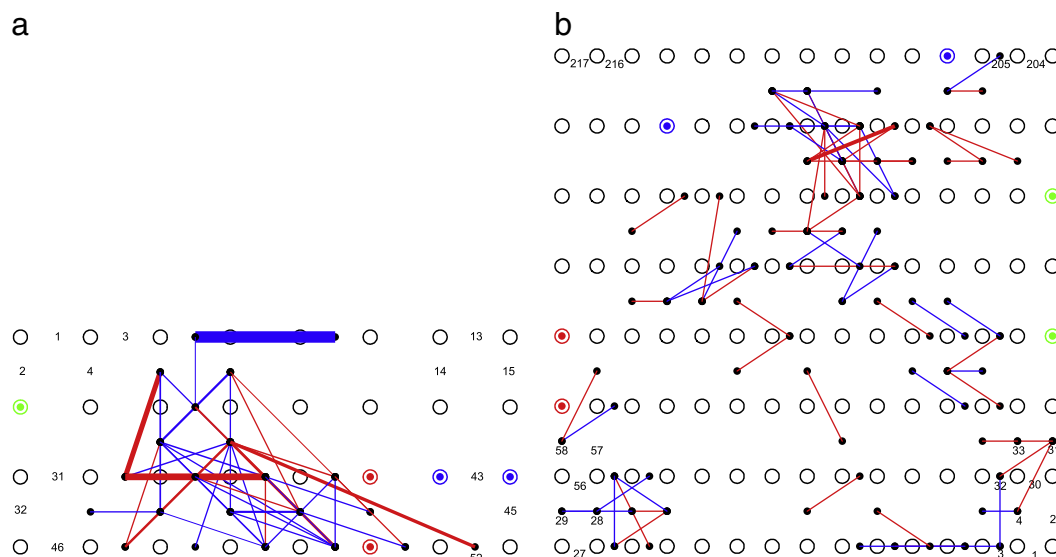


Fig. 7. Spatial pattern of increases (red lines) and decreases (blue lines) in synchrony observed when comparing (a) periods of sleep and wake for Patient 1 and (b) periods of low and high interictal discharge rates for Patient 2. In (a) and (b) hollow black circles represent electrode positions. Small solid black disks indicate the effective positions of differential montage channels, corresponding to the analysis in Fig. 6. The thicker the lines, which indicate increases or decreases in synchrony, the greater the change in synchrony between the periods of sleep and wake states, or low and high discharge rates. The electrodes marked in red, green and blue, correspond to the epileptic foci, recording references, and stimulation electrodes, respectively. The numbers indicate the pattern of differential montage channel numbering which also correspond to the channel numbers in Figs. 4(a), (b), and 5(a) and (b).

providing evidence that the use of an input stimulus may improve seizure anticipation algorithms.

The current study extends the work of Kalitzin et al. [19]; these authors used steady-state EEP responses from the mesial temporal lobe using periodic stimulation, whereas we use repetitive single pulse stimuli delivered to the neocortex. This may have an advantage with a reduced amount of charge delivered to the brain. The study can also be considered an extension of the work of Badawy et al. [26], which employed non-invasive TMS to primary motor cortex to track cortical excitability in epilepsy patients. Our electrical stimuli can be targeted directly at the epileptic focus, and therefore a more local measure of excitability of direct relevance to the epileptogenic tissue can be estimated.

A major benefit in using an ensemble of single pulse inputs to track cortical excitability over passive techniques is the ability to average the responses to improve the signal-to-noise ratio (SNR). The improved SNR overcomes a major difficulty in analyzing spontaneous EEG, where it is difficult to elucidate whether fluctuations in extracted features are due to changes in excitability, spurious fluctuations from normal brain processes, or even noise.

A possible concern when using electrical stimulation for measuring excitability is safety. This issue was raised in response to the Kalitzin study [38]. In this regard, the authors would like to point out that the patients did not have any percept of the stimulus at any time during the experiments (including other studies not reported in this paper). Further to this, the amount of charge delivered with the single pulse paradigm is less than scheduled therapeutic stimulators (see [39] for example). Histological studies of the resected specimens from the patients did not show abnormalities related to excessive charge delivery around the electrode contacts.

In diametric contrast to the safety issues surrounding electrical probing, a possible confound for using iEEG responses to low frequency stimulation for estimating cortical excitability is the potential therapeutic benefit of the approach [40,41]. It is thought that repetitive low frequency stimulation may induce long-term depression of cortical circuits, thereby decreasing cortical excitability and seizure frequency [42]. Therefore, the estimated cortical excitability levels may

be altered by the stimuli making it difficult to elucidate mechanisms that lead to seizures from iEEG features.

Interestingly, the MPV provided a more distributed feature than EEP amplitude. This is desirable for developing a seizure predictor, as the method is likely to be less sensitive to the stimulation location. An advantage of the MPV over the PLV is the ability to average over channels. Since there are widespread increases and decreases in the bivariate synchrony levels that do not appear to follow a spatial pattern, the PLV feature cannot be averaged. The apparent disorganized spatial patterns of the increases and decreases in synchrony were also observed in the study of Kuhlmann et al. [9], who used passive iEEG for seizure prediction.

The MPV feature was at a minimum at the time of the seizure in Patient 1, but was at a maximum when the epileptic discharge rate was at the peak for Patient 2. At first impression, this seems to be a confounding result. However, this may result from the stimulation location, where Patient 1 had stimuli delivered to the epileptic focus and Patient 2 had stimuli delivered to a more remote brain region. Nevertheless, the results from the MPV analysis showed a gradual change leading to the seizure. Although we are only considering a single clinical seizure in this study, this exciting result provides a proof-of-principle for our probing method of measuring excitability for seizure anticipation.

The results for Patient 2 showed that the features varied with the epileptic discharge rate without the occurrence of seizures. This provides evidence that changes in excitability may not be a sufficient condition for seizures. However, a change in excitability may lead to a higher likelihood of seizures. This has implications for the standard seizure prediction framework, where false positives are penalized. These false positives may reflect a state of increased seizure likelihood. There are two points to note regarding this statement. First, it may be more pragmatic to measure seizure likelihood rather than predict seizures. Second, methods that aim to predict seizures need to take into account cortical excitability and the likelihood of having a seizure based on the non-stationary statistics of the EEG or EEPs. Moreover, this should be done in consideration of how these changes may occur with respect to the time of day.

The authors hope that this paper motivates further research into uncovering when, how, and where we should stimulate the brain to uncover the normally hidden dynamics associated with subtle epileptic oscillations. We believe the amount of measurable information in the iEEG can be greatly improved by directing research down this path. Establishing a framework where it is possible to use electrical stimuli to interact with the neurodynamics also opens the door to applying well established techniques from systems engineering to forge a better understanding of the human brain. By using input–output system identification techniques it may be possible to construct models of the brain that will facilitate robust tracking of changes in critical parameters that lead to seizures [43,44]. Furthermore, construction of such models may lead to the application of robust controls to prevent the occurrence of pathologic oscillations that lead to seizures.

Conflict of interest statement

None of the authors have a conflict of interest.

Acknowledgments

The authors would like to thank the patients who participated in this study. The Bionics Institute acknowledges the support it receives from the Victorian State Government through the Operational Infrastructure Support Program. The authors would also like to acknowledge the L.E.W. Carty Charitable Fund for supporting this research.

References

- [1] Babloyantz A, Destexhe A. Low-dimensional chaos in an instance of epilepsy. *Proc Natl Acad Sci U S A* 1986;83(10):3513–7.
- [2] Pijn J, Van Neerven J, Noest A, Lopes da Silva F. Chaos or noise in EEG signals; dependence on state and brain site. *Electroencephalogr Clin Neurophysiol* 1991;79(5):371–81.
- [3] Pritchard W, Duke D. Measuring chaos in the brain—a tutorial review of EEG dimension estimation. *Brain Cogn* 1995;27(3):353–97.
- [4] Iasemidis L, Sackellares J. Chaos theory and epilepsy. *Neuroscientist* 1996;2(2):118–25.
- [5] Le Van Quyen M, Martinerie J, Baulac M, Varela F. Anticipating epileptic seizures in real time by a non-linear analysis of similarity between EEG recordings. *Neuroreport* 1999;10(10):2149–55.
- [6] Wendling F, Bartolomei F, Bellanger JJ, Bourien J, Chauvel P. Epileptic fast intracerebral EEG activity: evidence for spatial decorrelation at seizure onset. *Brain* 2003;126:1449–59 [0006–8950 Part 6].
- [7] Mormann F, Kreuz T, Andrzejak RG, David P, Lehnertz K, Elger CE. Epileptic seizures are preceded by a decrease in synchronization. *Epilepsy Res* 2003;53(3):173–85.
- [8] Le Van Quyen M, Soss J, Navarro V, Robertson R, Chavez M, Baulac M, et al. Preictal state identification by synchronization changes in long-term intracranial EEG recordings. *Clin Neurophysiol* 2005;116(3):559–68 [tY - JOUR].
- [9] Kuhlmann L, Freestone D, Lai A, et al. Patient-specific bivariate-synchrony-based seizure prediction for short prediction horizons. *Epilepsy Res* 2010;91(2–3):214–31.
- [10] Mormann F, Andrzejak R, Elger C, Lehnertz K. Seizure prediction: the long and winding road. *Brain* 2007;130(2):314.
- [11] Lehnertz K, Mormann F, Osterhage H, et al. State-of-the-art of seizure prediction. *J Clin Neurophysiol* 2007;24(2):147–53.
- [12] Scheffer M, Bascompte J, Brock W, et al. Early-warning signals for critical transitions. *Nature* 2009;461(7260):53–9.
- [13] Penfield W, Boldrey E. Somatic motor and sensory representation in the cerebral cortex of man as studied by electrical stimulation. *Brain* 1937;60(4):389.
- [14] Valentin A, Anderson M, Alarcon G, et al. Responses to single pulse electrical stimulation identify epileptogenesis in the human brain in vivo. *Brain* 2002;125(8):1709.
- [15] Valentin A, Alarcon G, Garcia-Seoane J, et al. Single-pulse electrical stimulation identifies epileptogenic frontal cortex in the human brain. *Neurology* 2005;65(3):426.
- [16] Valentin A, Alarcón G, Honavar M, et al. Single pulse electrical stimulation for identification of structural abnormalities and prediction of seizure outcome after epilepsy surgery: a prospective study. *Lancet Neurol* 2005;4(11):718–26.
- [17] Flanagan D, Valentin A, García Seoane J, Alarcón G, Boyd S. Single-pulse electrical stimulation helps to identify epileptogenic cortex in children. *Epilepsia* 2009;50(7):1793–803.
- [18] Kalitzin S, Parra J, Velis D, Lopes da Silva F. Enhancement of phase clustering in the EEG/MEG gamma frequency band anticipates transitions to paroxysmal epileptiform activity in epileptic patients with known visual sensitivity. *IEEE Trans Biomed Eng* 2002;49(11):1279–86.
- [19] Kalitzin S, Velis D, Suffczynski P, Parra J, da Silva F. Electrical brain-stimulation paradigm for estimating the seizure onset site and the time to ictal transition in temporal lobe epilepsy. *Clin Neurophysiol* 2005;116:718–28.
- [20] David O, Wozniak A, Minotti L, Kahane P. Preictal short-term plasticity induced by intracerebral 1 Hz stimulation. *Neuroimage* 2008;39(4):1633–46.
- [21] David O, Bastin J, Chabardès S, Minotti L, Kahane P. Studying network mechanisms using intracranial stimulation in epileptic patients. *Front Syst Neurosci* 2010;4:1–10.
- [22] Suffczynski P, Kalitzin S, da Silva F, Parra J, Velis D, Wendling F. Active paradigms of seizure anticipation: computer model evidence for necessity of stimulation. *Phys Rev E* 2008;78(5):51917.
- [23] O'Sullivan-Greene E, Mareels I, Burkitt A, Kuhlmann L. Observability issues in networked clocks with applications to epilepsy. *Proceedings of the 48th IEEE Conference on Decision and Control, 2009 held jointly with the 2009 28th Chinese Control Conference. CDC/CCC 2009; 2009. p. 3527–32.*
- [24] O'Sullivan-Greene E, Mareels I, Freestone D, Kuhlmann L, Burkitt A. A paradigm for epileptic seizure prediction using a coupled oscillator model of the brain. *Annual International Conference of the IEEE Engineering in Medicine and Biology Society, 2009. EMBC 2009; 2009. p. 6428–31.*
- [25] Kalitzin S, Velis D, Lopes da Silva F. Stimulation-based anticipation and control of state transitions in the epileptic brain. *Epilepsy Behav* 2010;17(3):310–23.
- [26] Badawy R, Macdonell R, Jackson G, Berkovic S. The peri-ictal state: cortical excitability changes within 24 h of a seizure. *Brain* 2009;132(4):1013–21.
- [27] Lin YY, Hsiao FJ, Shih YH, et al. Plastic phase-locking and magnetic mismatch response to auditory deviants in temporal lobe epilepsy. *Cereb Cortex* 2007;17(11):2516–25 [1047–3211].
- [28] Zhao M, Suh M, Ma H, Perry C, Geneslaw A, Schwartz T. Focal increases in perfusion and decreases in hemoglobin oxygenation precede seizure onset in spontaneous human epilepsy. *Epilepsia* 2007;48(11):2059–67.
- [29] Federico P, Abbott D, Briellmann R, Harvey A, Jackson G. Functional MRI of the pre-ictal state. *Brain* 2005;128(8):1811.
- [30] Vonck K, Boon P, Achten E, De Reuck J, Caemaert J. Long-term amygdalohippocampal stimulation for refractory temporal lobe epilepsy. *Ann Neurol* 2002;52(5):556–65.
- [31] Kerrigan J, Litt B, Fisher R, et al. Electrical stimulation of the anterior nucleus of the thalamus for the treatment of intractable epilepsy. *Epilepsia* 2004;45(4):346–54.
- [32] Kuncel A, Grill W. Selection of stimulus parameters for deep brain stimulation. *Clin Neurophysiol* 2004;115(11):2431–41.
- [33] Velasco A, Velasco F, Velasco M, Trejo D, Castro G, Carrillo-Ruiz J. Electrical stimulation of the hippocampal epileptic foci for seizure control: a double-blind, long-term follow-up study. *Epilepsia* 2007;48(10):1895–903.
- [34] Makeig S, Westerfield M, Jung T, et al. Dynamic brain sources of visual evoked responses. *Science* 2002;295(5555):690.
- [35] Heffer L, Fallon J. A novel stimulus artifact removal technique for high-rate electrical stimulation. *J Neurosci Methods* 2008;170(2):277–84.
- [36] Rosenblum M, Pikovsky A, Kurths J. Synchronization approach to analysis of biological systems. *Fluct Noise Lett* 2004;4:L53–62.
- [37] Fisher N. Statistical analysis of circular data. Cambridge University Press; 1996.
- [38] Osorio I. Electrical stimulation to assess brain dynamics and the probability of inter-ictal to ictal transitions could give Penfield and Heisenberg “fits”. *Clin Neurophysiol* 2005;117:695–6.
- [39] Velasco A, Velasco F, Velasco M, María N, Trejo D, García I. Neuromodulation of epileptic foci in patients with non-lesional refractory motor epilepsy. *Int J Neural Syst* 2009;19(3):139.
- [40] Yamamoto J, Ikeda A, Satow T, et al. Low-frequency electric cortical stimulation has an inhibitory effect on epileptic focus in mesial temporal lobe epilepsy. *Epilepsia* 2002;43(5):491–5.
- [41] Chen R, Classen J, Gerloff C, et al. Depression of motor cortex excitability by low-frequency transcranial magnetic stimulation. *Neurology* 1997;48(5):1398–403.
- [42] Barrionuevo G, Schottler F, Lynch G. The effects of repetitive low frequency stimulation on control and “potentiated” synaptic responses in the hippocampus. *Life Sci* 1980;27(24):2385.
- [43] Ullah G, Schiff S. Assimilating seizure dynamics. *PLoS Comput Biol* 2010;6(5):35–45.
- [44] Freestone D, Aram P, Dewar M, Scerri K, Grayden D, Kadirkamanathan V. A data-driven framework for neural field modeling. *Neuroimage* 2011:143–58.